ACS Sustainable Chemistry & Engineering

pubs.acs.org/journal/ascecg

Research Article

Uncovering the Phytochemical Basis and the Mechanism of Plant Extract-Mediated Eco-Friendly Synthesis of Silver Nanoparticles Using Ultra-Performance Liquid Chromatography Coupled with a Photodiode Array and High-Resolution Mass Spectrometry

Matam Pradeep, Dariusz Kruszka, Piotr Kachlicki, Dibyendu Mondal, and Gregory Franklin*

Cite This: *ACS Sustainable Chem. Eng.* 2022, 10, 562−571

Read Online

ACCESS | Metrics & More | Article Recommendations | Supporting Information

ABSTRACT: Plant extract is a complex concoction of several phytochemicals, for instance, phenolics, sugars, flavonoids, xanthones, and several others. In general, it is said that hydroxyl-rich phenolics act as reducing agents for metal ions, but little is discussed about the stabilizing ligands of metal nanoparticles (NPs). Thus, despite the popularity of plant extract-mediated synthesis of NPs, the phytochemical basis of the process and the exact mechanism are still unclear. Herein, a systematic study was carried out to unveil the mechanism of St. John's wort (*Hypericum perforatum* (*H. perforatum*) L.) extract-mediated synthesis of silver (Ag) NPs. Among the phytochemicals present in the extract, phenolic acids and flavonoids are shown to be involved in the reduction of Ag^+ ions, while xanthones and phloroglucinols act as capping agents, and naphthodianthrones were involved in both steps. Analysis of the postreaction residues by ultra-performance liquid chromatography coupled with a photodiode array and high-resolution mass spectrometry showed a sharp decrease in the concentration of various secondary metabolites present in the extract, of which large amounts of xanthones and phloroglucinols were recovered from the NPs. Consequently, the low polar fraction of *H. perforatum* extract, rich in xanthones and phloroglucinols, and the pure compounds of these classes (mangiferin and hyperforin) did not reduce Ag^+ ions. In contrast, the polar fraction of the extract, rich in flavonoids and naphthodianthrones, and the pure compounds of these classes (kaempferol-3-glucoside, quercetin, quercetin-3-glucoside, hypericin, pseudohypericin, and protohypericin) were able to reduce Ag^+ ions. Overall, the present study contributes significantly to the understanding of green synthesis of NPs by plant extracts.

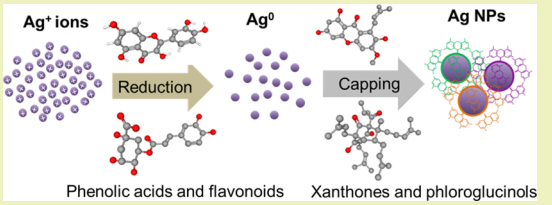

KEYWORDS: *plant extract, Hypericum perforatum L., phytochemicals, green synthesis, silver nanoparticles, mechanism*

INTRODUCTION

An exponential increase of the application of engineered nanoparticles (NPs) in various fields such as materials science, biomedicine, engineering, food, agriculture, and consumer product industries is currently witnessed. NPs are colloidal materials with a size below 100 nm in diameter.[1] Compared to their bulk forms, NPs exhibit distinct physicochemical and biological properties and better functionalities useful for industrial applications due to their high surface-to-volume ratio.[2,3] Reduction of metal ions in a dissolved state using chemical agents *via* a redox reaction forms the basis of chemical synthesis of NPs.[4,5] The size and shape of NPs could be controlled in chemical methods by tuning the reaction environment and reactants.[6] Despite these advantages, green synthesis of NPs using plant extracts is emerging as an attractive alternative to chemical methods from an environmental standpoint,[7−9] and several reports in this context can be pointed out.[10−15]

The absence of harmful chemicals in the process, environmental friendliness, simplicity of the procedures, huge availability of raw materials, and low cost of synthesis make the plant extract-mediated green synthesis of NPs a superior method compared to its counterparts. Furthermore, NPs synthesized using plant extracts are shown to be more biocompatible and biologically active than the ones synthesized *via* chemical methods.[16−18] Although a clear understanding of phytochemicals involved in the green synthesis of NPs would help us to devise new strategies to control the physicochemical properties such as size and shape of NPs, it remains challenging due to the complexity of plant extracts.

Plant extracts consist of several biomolecules belonging to various structural classes such as alkaloids, polysaccharides, vitamins, amino acids, proteins, enzymes, tannins, phenolic acids, saponins, terpenoids, etc. According to various studies, most of these molecules were predicted to participate in the

Received: October 16, 2021
Revised: December 9, 2021
Published: December 16, 2021

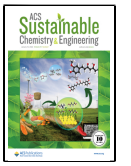

green synthesis of NPs, and Fourier transform infrared spectroscopy (FT-IR) has been generally applied to follow the green synthesis processes.[8] However, there are many uncertainties, for instance, sitoindoside was identified as a potential capping and stabilizing agent in *Withania somnifera* extract-mediated synthesis of Ag NPs by the presence of an IR band corresponding to the geminal dimethyl group in the FT-IR spectra.[19] However, high-performance liquid chromatography (HPLC) analysis of the compounds eluted from the corresponding Ag NPs revealed the presence of catechin, *p*-coumaric acid, luteolin-7-glucoside, and a withanolide derivative as the capping agents.[17]

Similarly, quercetin was suggested as the compound mainly responsible for the reduction of Ag^+ ions in the *Ocimum sanctum* (*O. sanctum*) leaf extract based on the similarities between the Ag NPs synthesized using leaf extract and pure quercetin in terms of optical, morphological, and antibacterial properties.[20] Nevertheless, the presence of terpenoids, flavonoids, eugenol having functional groups like alcohols, phenols, amines, carboxylic acids, ethers, esters, etc. was revealed by FT-IR analysis in Ag NPs synthesized using *O. sanctum* leaf extract.[21] All the paradoxical observations clearly emphasize the complexity of elucidating the phytochemicals participating in the green synthesis process.

St. John's wort (*Hypericum perforatum* (*H. perforatum*) L.) is one of the most important medicinal plant species that possess unique classes of compounds (xanthones, phloroglucinols, naphthodianthrones, etc.), in addition to other common secondary metabolites, making this species an ideal candidate for the study aimed at understanding the role of phytochemicals in the green synthesis process. Herein, we analyzed the changes in the phytochemical profile of *H. perforatum* extract during the green synthesis of Ag NPs, and the compounds eluted from the NPs by ultra-performance liquid chromatography coupled with a photodiode array and high-resolution mass spectrophotometry (UPLC-PDA-HRMS). Compounds predicted to participate in the process were tested for their ability to reduce Ag^+ ions *in vitro*. Overall, a detailed study to understand the phytochemical basis and the mechanism of *H. perforatum* extract-mediated synthesis of Ag NPs is disclosed envisaging controlled synthesis of NPs with concomitant purification of low polar plant components from complex plant extract.

EXPERIMENTAL SECTION

Materials. The aerial part of the *H. perforatum* plants just before flowering was collected at the Institute of Plant Genetics of the Polish Academy of Sciences campus (Poznan, Poland). The collected biomass was ground into fine powder using a mortar and pestle and dried by lyophilization under a vacuum pressure of 0.015 mbar in a freeze-dryer at −50 °C (Heto-Holten, Denmark). Silver nitrate ($AgNO_3$) was purchased from Sigma-Aldrich, Germany. All the solvents used in the study were of LC−MS grade (Sigma-Aldrich, Germany).

Preparation of Plant Extract. *H. perforatum* extracts used in the present study were prepared as follows. Briefly, 2.0 g of the powdered biomass was added into an Erlenmeyer flask containing 20 mL of 80% methanol (Sigma-Aldrich, Steinheim, Germany) and mixed well by shaking at 150 rpm for 1 h at 25 °C in an orbital shaker (ORBI-SHAKER XL, Benchmark Scientific, NJ, USA). The mixture was then subjected to sonication in an ultrasound water bath (Sonorex, Bandelin, Berlin, Germany) for 10 min, and the homogenate was centrifuged at 15,000*g* (J2-21MIE, JA-20 rotor, Beckman, UK) for 30 min. The supernatant was dried under vacuum at 35 °C in a rotary evaporator (BuchiR114), and the resulting residue was dissolved in 100 mL of ultrapure water to obtain a turbid 2% *H. perforatum* aqueous methanolic extract (TE). The TE (50 mL) was centrifuged at 15,000*g* (J2-21MIE, JA-20 rotor, Beckman, UK) for 30 min. The supernatant containing the polar fraction (PF) of the aqueous methanolic extract was collected. The pellet was dissolved in 50 mL of methanol to obtain the low polar fraction (LPF).

Antioxidant Potential of Extracts. The antioxidant potential of TE, PF, and LPF was tested using 2,2-diphenyl-2-picrylhydrazyl (DPPH) reduction assay. Briefly, 50 μL of the extract was mixed with 1.45 mL of 160 μM DPPH dissolved in 96% ethanol taken in a 2.0 mL Eppendorf tube, and the absorbance at 515 nm was read continuously in a UV−vis spectrophotometer (PerkinElmer, Lambda2). The percentage of reduced DPPH at a steady state (DPPH-R) was calculated.

Green Synthesis of Silver Nanoparticles (Ag NPs). For Ag NPs' green synthesis, to 20 mL of 1 mM $AgNO_3$ (Sigma-Aldrich, Germany) taken in 50 mL volumetric flasks, 2 mL of different extracts (TE, PF, and LPF) was added and mixed vigorously on a vortex mixer at 3000 rpm (MS3, IKA, Germany) for 5 min. Then, the reaction mixtures were stirred continuously on a benchtop stirrer at 100 rpm at room temperature. Aliquots taken from the reaction mixtures were tested for the formation of Ag NPs by reading the absorption in a UV−vis spectrophotometer (UV-1800, Shimadzu, Kyoto, Japan) at 190−1000 nm with an increment of 1 nm. On day 5, the reaction mixtures were transferred to 50 mL Sorvall tubes and centrifuged at 48,384*g* (J2-21MIE, JA-20 rotor, Beckman, UK) for 30 min to pelletize the Ag NPs. Ag NP pellets and supernatants containing the postreaction residues were collected separately and dried by lyophilization.

Dried residues of various reactions were dissolved in 1 mL of methanol and stored at −20 °C for the UPLC analysis. Similarly, compounds adsorbed on the surface of Ag NPs were washed serially with LC−MS-grade solvents from high to low polarity, namely, water, methanol, ethanol, acetone and ethyl acetate, to recover the compounds. Briefly, 1 mL of the respective solvent was added to the dried Ag NP pellets, vortexed for 5 min, and sonicated in an ultrasound water bath (Sonorex, Bandelin, Berlin, Germany) for 15 min. Then, the mixture was centrifuged at 25,150*g* (Hettich EBA 21, 1024 rotor) at 20 °C for 30 min to pelletize the Ag NPs. After collecting the supernatant, the NPs were washed with the next solvent, and the supernatants were collected in the same manner.

Reduction of Ag^+ Ions Using Isolated Compounds. The Ag^+ ion reduction potential of pure standard compounds (Sigma-Aldrich, Germany) representing various classes of secondary metabolites present in the *H. perforatum* extract, namely, phenolic acids (vanillic acid and chlorogenic acid), flavonoids (kaempferol, kaempferol-3-glucoside, quercetin, quercetin-3-glucoside, and 3,8″-biapigenin), xanthones (mangiferin), phloroglucinols (hyperforin), and naphthodianthrones (hypericin, pseudohypericin, and protohypericin), was tested. Briefly, 500 μL of each compound containing a concentration equivalent to its presence in the RM was added to 500 μL of 10 mM $AgNO_3$, vigorously vortexed at 3000 rpm (MS3, IKA, Germany) for 5 min, and continuously shaken on a benchtop orbital shaker. The samples were continuously observed for the reduction of Ag^+ ions for 5 days.

Characterization of Ag NPs. Ag NPs were characterized by high-resolution transmission electron microscopy (HR-TEM) at an accelerating voltage of 100 kV (Hitachi, HT7700) after deposition of the NPs on carbon-coated copper grids. The hydrophobicity of Ag NPs was tested using water−octanol coefficients by a shake flask method. Briefly, 5 mL of the Ag NP water dispersion was mixed well with an equal volume of octanol by vortexing and maintaining it on a shaker for 1 h. Then, the partition of the NPs between water and octanol phases was observed.

Identification of Compounds. All the 41 compounds of aqueous total extract (TE) were analyzed by UPLC-PDA-HRMS. Samples were filtered through syringe filters (PTFE 13 mm, 0.45 μm discs, Kinesis KX, Vernon Hills, USA) into 2 mL glass vials (Agilent Technologies, Santa Clara, USA). The injection volume was 2 μL. Compounds were separated on a BEH C18 column (2.1 × 100 mm,

https://doi.org/10.1021/acssuschemeng.1c06960
ACS Sustainable Chem. Eng. 2022, 10, 562−571

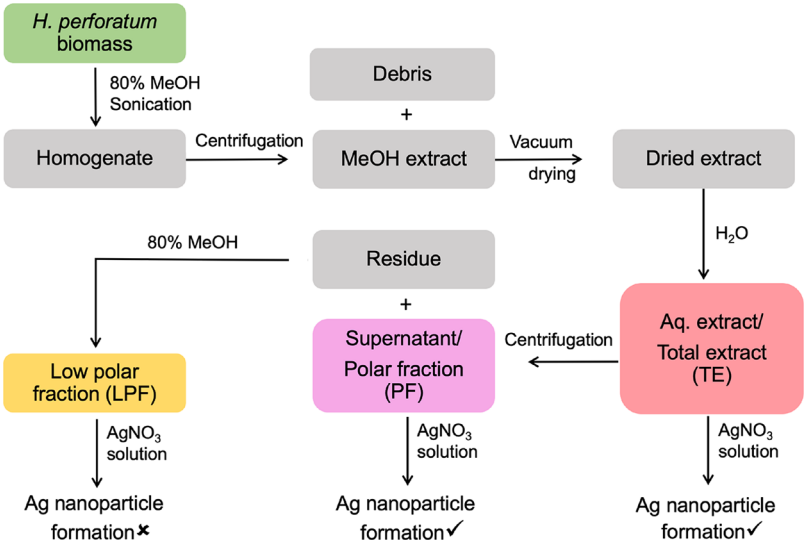

Figure 1. Schematic depiction of the overall process comprising preparation of different extracts and suitability of such extracts toward Ag nanoparticle formation.

1.7 μm, Waters) at a temperature of 50 °C using a binary gradient mobile phase consisting of (A) 10 mM ammonium acetate acidified with 0.1% formic acid in Millipore water and (B) acetonitrile/methanol (80:20) with a flow rate of 0.3 mL/min that was applied in the following gradient program: 0.0−0.5 min, 5% B; 0.5−2.0 min, 15% B; 2.0−6.0 min, 20%; 6.0−10.0 min, 60% B; 10.0−17.0 min, 99%; 17.0−19.0 min, 99%; 19.0−20.0 min, from 99% to 5% B. Chromatograms were recorded at 254, 270, 330, and 590 nm. The eluted compounds were analyzed using full MS and data-dependent scanning in negative mode for MS/MS analysis. The normalized collision energy (NCE) of the cell was 30% for the data-dependent scan. N_2 was employed as a sheath gas (35 arbitrary units), the sweep gas flow was 4 arbitrary units, and the auxiliary gas flow was 10 arbitrary units. Automatic gain control (AGC) was established as follows: maximum injection time, 100 ms; AGC target, 3e6; resolution for full MS, 70,000. Data-dependent scanning comprises a full MS scan in the range between 100 and 1000 m/z followed by a data-dependent scan at a resolution of 17,500. Xcalibur software (version 3.0.63) was used for instrument control, data acquisition, and data analysis. The identification of compounds was confirmed based on their exact masses, and structural formulas with ppm resolution of compound purity in negative ion mode are summarized in Supporting Information Table S1. The PubChem database with accurate mass spectrometry data and molecular characteristics was used as a reference library to identify compounds.

Quantification of Compounds. The above identified compounds were quantified in the *H. perforatum* extracts (TE, PF, and LPF), postreaction residues, and the Ag NP wash solutions by a UPLC Acquity system (Waters), equipped with a PDA detector. The samples (10 μL) were analyzed using the same method as described in the previous section. Chromatograms were recorded at 254 (phenolic acids, flavonoids, and xanthones), 270 (phloroglucinols), and 590 nm (naphthodianthrones). Peaks were identified based on their retention time (R_t) and quantified using external standards: pseudohypericin, hyperforin, quercetin-3-glucoside, chlorogenic acid, and mangiferin (Sigma-Aldrich, Steinheim, Germany). Wherever standards were not available for compounds belonging to flavonoids, phenolic acids, phloroglucinols, xanthone derivatives, and protopseudohypericin, they were quantified as the equivalents of quercetin-3-glucoside, chlorogenic acid, hyperforin, mangiferin, and pseudohypericin, respectively. Quantification of the identified compounds was performed in excel sheets based on peak areas with coefficient values of calibration curves (R^2 = 0.9934−0.9945).

RESULTS AND DISCUSSION

Aqueous extracts prepared by boiling or heating the biomass in water have been commonly used in the plant extract-mediated NP synthesis,[22−24] and in some of the recent studies, the biomass is simply mixed in water to obtain the aqueous extract. While boiling or heating can affect the stability of the compounds, many of the low polar compounds cannot be extracted in the latter methods. Figure 1 shows the methodology adopted in the present study to prepare different extracts from pristine biomass and their suitability toward preparation of Ag NPs. Since the present study is aimed at understanding the green synthesis process comprehensively, we extracted the total secondary metabolites in methanol, concentrated them by lyophilization, and resuspended them in water to obtain an aqueous methanolic extract (TE). In addition to the TE, its polar fraction (PF) and low polar fraction (LPF) were also tested for the green synthesis of Ag NPs. The complete experimental protocols for the preparation of different extracts and use of such extracts for the synthesis of Ag NPs are provided in the Experimental Section. The reaction mixtures containing the TE and PF showed a distinct change of color after addition of $AgNO_3$, whereas the one with the LPF did not show any significant change in color (Figure 2a). The color change of the reaction mixtures is indicative of the reduction of Ag^+ ions to their elemental form by the components present in the extract and the subsequent formation of Ag NPs.

While an equal efficiency of Ag NP synthesis was observed in the reactions performed using the TE and PF (Figure 2a), NPs were not formed, when the LPF was used in the reaction, indicating that polar compounds are participating in the reduction reaction. This observation was further proven by UV−vis analysis (Figure 2a). As can be seen from the spectra, a distinct band in between 400 and 450 nm (corresponding to the excitation of the surface plasmon vibration of colloidal silver NPs) is clearly visible for Ag NPs prepared using the TE and PF, but such a band is insignificant in the presence of the LPF even after 4 days of reaction time. Neither any absorption band with maxima at 450 nm nor any changes in the color were observed with the Ag^+ ion precursor and LPF during the

https://doi.org/10.1021/acssuschemeng.1c06960
ACS Sustainable Chem. Eng. 2022, 10, 562−571

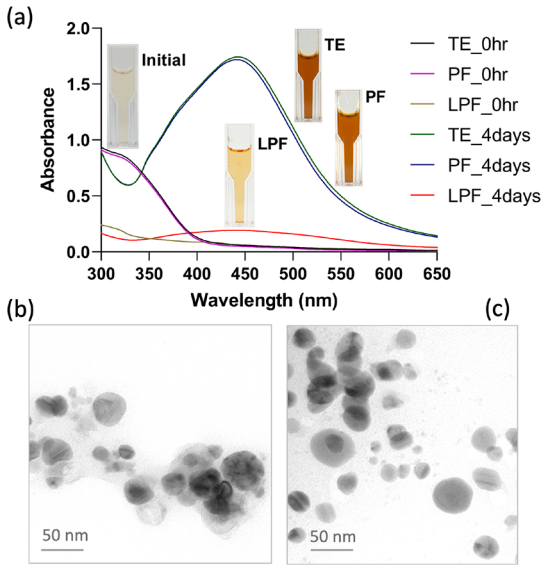

Figure 2. (a) UV−vis spectra of Ag NPs prepared at different time intervals using different extracts from biomass. Insets show the color changes of the reaction mixtures. (b) TEM image of Ag NPs prepared using TE and 1 mM $AgNO_3$. (c) TEM image of Ag NPs prepared using PF and 1 mM $AgNO_3$.

initial 12 h of reaction time. Meanwhile, with other fractions such as the TE and PF, Ag NP formation was found within 12 h (Figure S1). The reaction got saturated with the TE and PF after 4 days; thereafter, Ag NPs pellets were recovered for further study. Although there was a slight absorption band at 450 nm in the UV−vis spectrum (Figure 2a) for the LPF after 4 days, no Ag NP pellet was recovered even after centrifugation at 48,384*g*. Overall, with the sluggish reaction kinetics and unavailability of Ag NP pellets even after 4 days of the reaction, the possibility of Ag NP formation with the LPF was ruled out. The sizes of Ag NPs obtained using the TE and PF were analyzed by HR-TEM imaging, and Ag NPs with a size of ∼50 nm were observed (Figure 2b,c). To further strengthen the suitability of the TE and PF toward reduction of Ag^+ ions, an attempt was made to test the relationship between the antioxidant potential of different extracts and Ag^+ ion reduction by the DPPH reduction assay. The results revealed that the TE and PF are excellent sources of antioxidants and could reduce more than 50% of DPPH within a minute, whereas the LPF could reduce only about 13% after 20 min (Figure 3).

Generally, the ability of plant extracts to reduce metal ions into NPs is attributed to their antioxidant activities.[25−27] *H. perforatum* extract exhibits several pharmacological properties due to its antioxidant activities, which have been demonstrated in several studies.[28−33] Although various classes of compounds are present in the *H. perforatum* extract, its antioxidant capacities are generally attributed to the presence of xanthones, flavonoids, and phenolic acids.[29,33−36] In the LPF used in the present study, xanthones and phloroglucinols are the major compounds, and its low antioxidant potential suggests that these classes of compounds might have not participated in the Ag^+ ion reduction. The failure of xanthones to reach even 50% DPPH reduction was reported before.[37] The naphthodianthrone hypericin was also found to possess a low level of antioxidant potential.[32]

After successful synthesis and characterization of Ag NPs using different fractions of biomass extract, an effort was further made to elucidate the complex concoction of biomass extract and the phytochemical basis that is responsible for reduction and stabilization of Ag NPs. Although spectroscopic methods such as FT-IR are frequently used to predict the reducing and capping agents, the results may not be accurate, as the functional groups and bonds of interest might occur across several classes of phytochemicals. The analysis of compounds in the postreaction residues and the synthesized NPs by advanced chromatographic methods could provide more precise information about the molecules involved in the process. Accordingly, the phytochemical profiles of the TE, PF, and LPF were analyzed by LC−MS/UPLC-PDA. Based on the fragmentation pattern from LC−MS, 41 compounds belonging to phenolic acids, flavonoids, xanthones, phloroglucinols, and naphthodianthrones were identified in the TE (Table 1, Table S1, and Figure S2). Further, UPLC-PDA analysis of the extracts revealed the presence of both polar and low polar compounds in the TE, while most of the low polar compounds and polar compounds were found respectively in the LPF and PF of the TE (Figure 4).

When the postreaction residue or the supernatant after Ag NP preparation using the TE was analyzed, many of the phytochemicals recorded in the pristine TE were either present at lower concentrations than in the mother extract or absent. Many compounds such as kaempferol 3-*O*-arabinoside, 3,8″-biapigenin, gancaonin O (6-prenylluteolin), mangiferin, 1,3,5-trihydroxy-6-methoxyxanthone, 1,8-dihydroxy-3,5-dimethoxy-2-prenylxanthone, tomoeone E, 33-hydroperoxyfurohyperforin, hyperevolutin A, hyperforin, $C_{35}H_{50}O_5$ (phloroglucinol derivative 03), pseudohypericin, protohypericin, hypericin, etc.

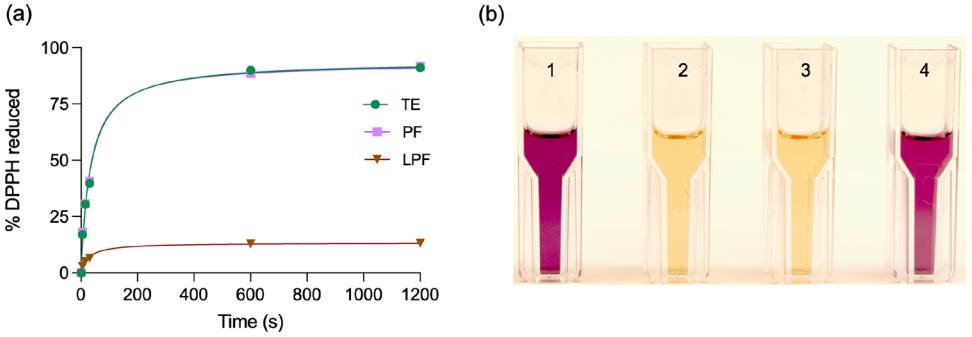

Figure 3. Graph showing the DPPH reduction potential of aqueous methanolic extract (TE), its polar fraction (PF), and low polar fraction (LPF) as a function of time (a) and DPPH reduction visualized in the blank (1), TE (2), PF (3), and LPF (4) samples after 20 s (b).

https://doi.org/10.1021/acssuschemeng.1c06960
ACS Sustainable Chem. Eng. 2022, 10, 562−571

Table 1. Details of the Peak Number (Pk), Retention Time (R_t), and Concentration of Secondary Metabolites Present in the Initial Reaction Mixture (RM), the Postreaction Supernatant (PS), and the Resulting Nanoparticles (NP) of the Reaction Performed Using 1 mM $AgNO_3$ and the TE

			amount (μg)		
Pk	R_t	compound	RM	PS	NP
1	2.07	vanillic acid glucoside	30.3 ± 4	3 ± 0.4	0
2	2.28	neochlorogenic acid (3-caffeoylquinic acid)	119 ± 4	12 ± 0.6	299 ± 1.6
3	2.74	chlorogenic acid (5-caffeoylquinic acid)	109 ± 5	9.4 ± 0.5	0
4	3.08	mysorenone A	126 ± 7	13 ± 0.7	0
		total phenolic acids	384 ± 14.5	37.1 ± 1	299 ± 1.6
6	4.8	miquelianin (quercetin 3-*O*-glucuronide)	362 ± 60	7.64 ± 0.6	0
7	5.38	quercetin-3-glucoside	1049 ± 33	43.2 ± 1.1	6.24 ± 0.7
9	6.14	avicularin (quercetin 3-*O*-α-L-arabinofuranoside)	65.9 ± 12	2.15 ± 0.2	0
8	5.76	quercetin 3-(2″-acetylgalactoside)	243 ± 19	9.12 ± 0.3	0
10	6.83	kaempferol 3-*O*-hexoside	186 ± 11	8.37 ± 0.7	5.31 ± 0.7
11	7.22	kaempferol 3-*O*-arabinoside	52.3 ± 6	0	2.86 ± 0.6
13	7.99	catechin-5-*O*-β-D-glucopyranoside	19.9 ± 6	8.88 ± 0.4	5.26 ± 1.1
17	9.43	3,8″-biapigenin	1.99 ± 0.1	0	0
22	11.21	gancaonin O (6-prenylluteolin)	3.47 ± 0.4	0	0
		total flavonoids	1984 ± 53	79.4 ± 1.4	19.7 ± 2.3
5	3.44	mangiferin	125 ± 12	0	0
18	9.59	1,3,5-trihydroxy-6-methoxyxanthone	58.4 ± 12	0	23.8 ± 3.8
15	9.10	hyperxanthone F	160 ± 8	1.76 ± 0.1	32.1 ± 2.1
14	8.01	1,3,5,6-tetrahydroxyxanthone	8.07 ± 1	0.01 ± 0	0
12	7.94	1,3-dihydroxy-2-methoxyxanthone	11 ± 1	0.11 ± 0.01	0
19	10.01	cadensin G (xanthone)	10.9 ± 0.4	0.17 ± 0.01	0.8 ± 0.1
16	9.37	1,3,7-trihydroxyxanthone	7.8 ± 2	0	2.33 ± 0.3
21	11.05	1,3,7-trihydroxy-6-methoxy-8-prenylxanthone	451 ± 10	16.4 ± 1	954 ± 14
25	11.9	paxanthone	37.2 ± 4	1.22 ± 0.1	94.5 ± 5
23	11.46	1,3,5,6-tetrahydroxy-2-(3-methylbut-2-enyl)xanthone	56.3 ± 5	1.87 ± 0.1	25.9 ± 1.7
24	11.66	calycinoxanthone D	33.6 ± 8	1.03 ± 0.1	41.2 ± 2.3
29	12.70	paxanthonin	12.7 ± 5	0.95 ± 0.1	44.1 ± 3.4
28	12.53	xanthone	12.2 ± 3	0.98 ± 0.1	43.5 ± 5.2
20	10.54	1,8-dihydroxy-3,5-dimethoxy-2-prenylxanthone	5.61 ± 1	0	0.91 ± 0.1
		total xanthones	990 ± 15	24.5 ± 1.2	1263 ± 15
30	13.85	tomoeone E	20.9 ± 9	0	28.6 ± 6.2
32	14.98	papuaforin C	8.11 ± 4	0.23 ± 0.01	11.9 ± 2.2
33	15.02	33-hydroperoxyfurohyperforin	7.11 ± 1	0	3.57 ± 1.5
39	16.29	furohyperforin	12.8 ± 1	0	11.3 ± 2
37	15.56	phloroglucinol derivative 01	15.6 ± 1	0.17 ± 0.01	20.7 ± 2.9
38	15.72	phloroglucinol derivative 02	21.3 ± 1	0.18 ± 0.01	17.4 ± 0.9
36	15.26	hyperevolutin A	300 ± 14	0	17.2 ± 3.1
40	16.50	hyperforin	49.7 ± 3	0	4.66 ± 1.6
41	16.73	adhyperforin	13.2 ± 1	0	28.3 ± 2.6
34	15.18	phloroglucinol derivative 03	9.68 ± 2	0	0.89 ± 0.1
		total phloroglucinols	458 ± 21	0.58 ± 0.07	145 ± 4.9
26	11.94	protopseudohypericin	4.88 ± 0.1	0	0.15 ± 0.01
27	12.39	pseudohypericin	22.1 ± 2	0	3.92 ± 0.7
31	14.52	protohypericin	1.35 ± 0.1	0	0.72 ± 0.1
35	15.19	hypericin	0.76 ± 0.1	0	1.32 ± 0.4
		total naphthodianthrones	29.1 ± 1.5	0	6.11 ± 0.7

were exhausted in the postreaction residues (Table 1). The area of peaks representing these compounds was also decreased (Figure 5). To know the phytochemicals that participated/were exhausted from the TE during Ag NP formation, the Ag NPs were recovered and were serially washed with many solvents (MeOH, EtOH, EtOAC, and acetone).

The UPLC chromatogram for methanol-washed Ag NPs is depicted in Figure 5, whereas the chromatograms for other solvent-washed Ag NPs are provided in Figure S3. In all cases, the eluates of Ag NPs showed the presence of peaks corresponding to compounds that were either depleted or found at reduced concentrations in the postreaction residues (Figure 5 and Table 1). These compounds are the putative capping agents, whereas compounds that were not present in these eluates and were reduced or depleted in the postreaction residues might have acted as reducing agents. Some of the compounds that disappeared from the postreaction supernatant were found in at least one of the Ag NP eluates (Table 1). On the other hand, some compounds actually present in

https://doi.org/10.1021/acssuschemeng.1c06960
ACS Sustainable Chem. Eng. 2022, 10, 562−571

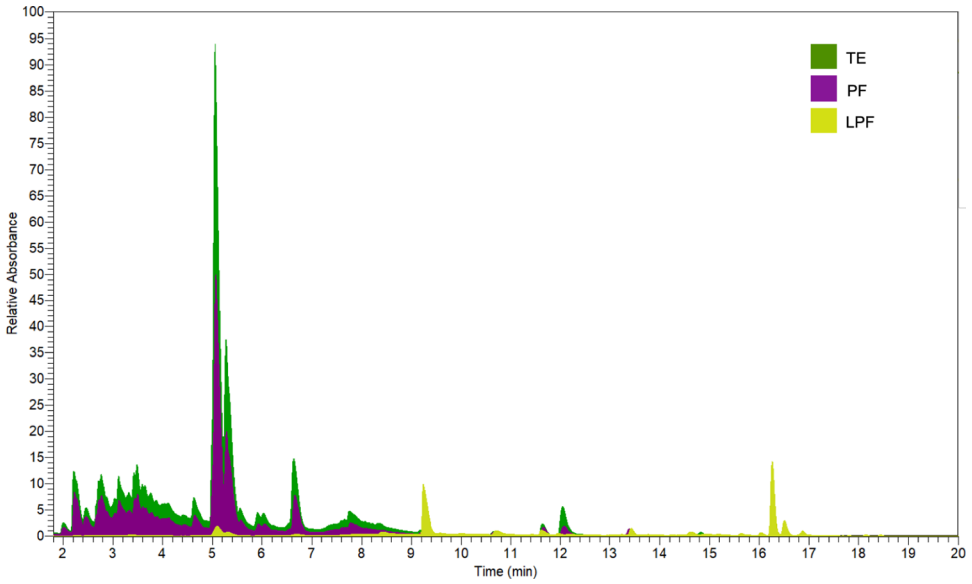

Figure 4. Chromatograms of the *H. perforatum* aqueous extract (TE), the polar fraction (PF), and the low polar fraction (LPF) recorded in the UPLC-PDA channel at a 270 nm absorbance.

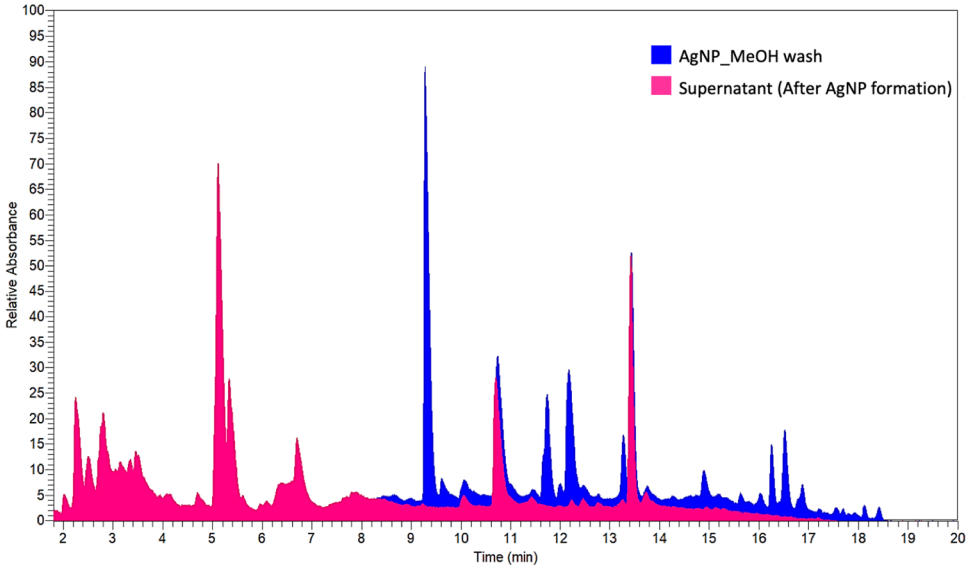

Figure 5. Chromatograms of the postreaction supernatant and phytochemicals eluted in methanol from Ag NPs synthesized using 1 mM $AgNO_3$ and TE. The spectra were recorded in the UPLC-PDA channel at a 270 nm absorbance.

low concentrations in the residues, such as vanillic acid glucoside, chlorogenic acid (3-caffeoylquinic acid), mysorenone A, miquelianin (quercetin 3-*O*-glucuronide), gancaonin O, and 1,3-dihydroxy-2-methoxyxanthone, were not found in these eluates. Despite the absence of chlorogenic acid (3-caffeoylquinic acid), its isomer neochlorogenic acid (5-caffeoylquinic acid) was found at a higher concentration than that of the extract in the eluates. Incubation of chlorogenic acid with green synthesized Ag NPs resulted in its conversion to neochlorogenic acid bound to the NPs, suggesting that the former may have been converted to the latter by an isomerization reaction catalyzed by the surface plasmon resonance of the Ag NPs.[38] Moreover, the neochlorogenic acid bound to the NPs could only be eluted with the least polar solvent, namely, ethyl acetate (Figure S3), but not with other solvents used in this study, suggesting that the binding of this compound with the Ag NPs might be strong. Another series of compounds found in small amounts in the residues, such as quercetin-3-glucoside, avicularin (quercetin derivative), quercetin 3-(2″-acetylgalactoside), kaempferol 3-*O*-hexoside, 1,2,4,5-tetrahydroxy-7-(hydroxymethyl)-9,10-anthraquinone, kaempferol 3-*O*-arabinoside, etc., were also obtained in small amounts from the Ag NP washing solutions. It is possible that these compounds were used as reducing and (or) capping agents in the reaction.

To understand the phytochemicals participating in the reduction process, standard compounds representing different classes of secondary metabolites present in the TE were tested for their Ag^+ ion reduction potential. Phenolic acid, namely, chlorogenic acid, flavonoids, such as kaempferol-3-glucoside, quercetin, and quercetin-3-glucoside, and all the tested naphthodianthrones (hypericin, pseudohypericin, and protohypericin) were able to reduce Ag^+ ions. Nevertheless, phenolic acid like vanillic acid and flavonoids such as

https://doi.org/10.1021/acssuschemeng.1c06960
ACS Sustainable Chem. Eng. 2022, 10, 562−571

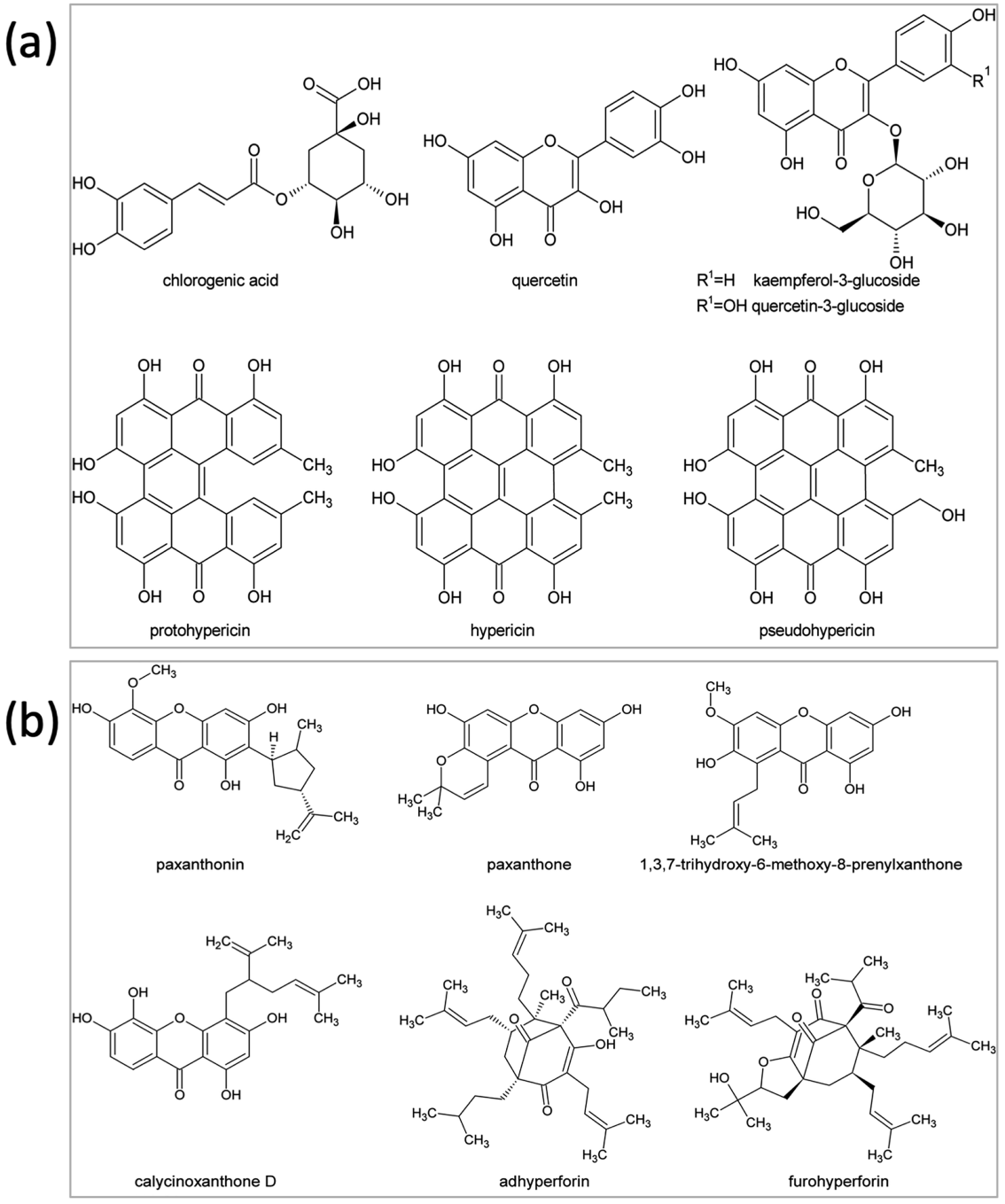

Figure 6. (a) Structural formulas of compounds involved in the reduction of Ag^+ ions and (b) structural formulas of selected compounds involved in the capping action.

kaempferol and 3,8″-biapigenin did not perform the reaction. The tested phloroglucinol (hyperforin) and xanthone (mangiferin) failed to reduce Ag^+ ions. Previous studies have shown that kaempferol,[39] chlorogenic acid,[40] quercetin,[20] apigenin,[41] and kaempferol glucoside[42] were able to reduce metal ions such as Au^{3+}. ZnO NPs were synthesized using rutin, when the reaction mixture was pH-adjusted to 12 and stirred at 60 °C.[43] Isolated flavonoids have been reported to participate in green synthesis under various pH and temperature conditions based on FT-IR spectral data.[20,39−41,43] Most of the studies reported the same molecule as both reducing and capping agents. Involvement of the polar hydroxyl groups of apigenin in reducing and capping the Au NPs has been predicted.[41] Kaempferol molecules acted as both reducing and stabilizing agents.[39] Similarly, rutin was shown to perform both the reduction and capping functions in the synthesis of ZnO NPs.[43] Analysis of the phenolic profile before and after green synthesis of Ag and Au NPs using *Eucalyptus globulus* bark extract by HPLC revealed that gallic acid and galloyl derivatives were mainly responsible for the reduction.[24] The major reducing agents in the *H. perforatum* extract-mediated green synthesis of Ag NPs are seen in Figure 6a. Interestingly, some compounds that were present in very low concentrations or absent in the postreaction supernatant compared to the extract were 1,3,5-trihydroxy-6-methoxyxanthone, hyperxanthone F, 1,3,5,6-tetrahydroxyxanthone, cadensin G, 1,3,7-

https://doi.org/10.1021/acssuschemeng.1c06960
ACS Sustainable Chem. Eng. 2022, 10, 562−571

trihydroxyxanthone, 1,3,7-trihydroxy-6-methoxy-8-prenylxanthone, paxanthone, 1,3,5,6-tetrahydroxy-2-(3-methylbut-2-enyl)xanthone, calycinoxanthone D, paxanthonin, xanthone, tomoeone E, papuaforin C, 33-hydroperoxyfurohyperforin, furohyperforin, $C_{31}H_{46}O_4$ (phloroglucinol derivative 01), $C_{27}H_{40}O_4$ (phloroglucinol derivative 02), hyperevolutin A, hyperforin, and adhyperforin. These compounds were recovered in significant amounts from the Ag NP eluates. Although most of the above xanthones were found in the Ag NPs, 1,3-dihydroxy-2-methoxyxanthone was not seen. Similarly, mangiferin was found only in trace amounts in the washing solutions compared to its original concentration provided in the reaction mixture (Table 1). Despite the absence of naphthodianthrones (protopseudohypericin, pseudohypericin, protohypericin, and hypericin) in the supernatant, they were also recovered in significant amounts from the Ag NPs. Since most of the above low polar compounds like xanthones, phloroglucinols, naphthodianthrones, etc. were recovered in significant amounts from the Ag NPs, these compounds might act as capping or stabilizing agents of Ag NPs. In this context, the better bioactivities of the green synthesized NPs reported in previous studies could be attributed to the presence of low polar compounds on the surface of these NPs.[17,44] The major capping agents in the *H. perforatum* extract-mediated green synthesis of Ag NPs are shown in Figure 6b.

Based on the results obtained above, a plausible mechanistic model for *H. perforatum* extract-mediated green synthesis of Ag NPs is depicted in Figure 7. Due to the antioxidant potential of

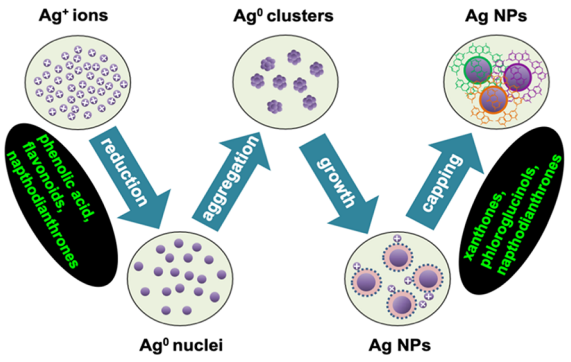

Figure 7. Putative model for the *H. perforatum* extract-mediated green synthesis of Ag NPs.

the phenolic acids, flavonoids, naphthodianthrones, etc. present in the extract, the Ag^+ ions in the dissolved state are rapidly reduced to Ag^0 as soon as the extract is added to aqueous $AgNO_3$ solution. Once reduced, the atomic nuclei tend to cluster together starting the process of NP formation. Once the maximum size is reached, the hydrophobicity of the NPs attracts the capping agents onto their surface to stabilize the surface energy. The common feature of all the predicted reducing agents is the presence of an enol group, while the presence of methoxy and/or prenyl groups is the common feature of the putative capping agents. Previous studies have also shown the withanolide derivative and isorhamnetin both containing methyl groups as capping agents.[17,24] In general, for the compound to act as a reducing agent, it requires an enol group, while for it to act as a capping agent, it requires a methyl group. If the compounds possess both groups, then they can perform dual functions.

CONCLUSIONS

In summary, a well-ordered study was undertaken to expose the phytochemical basis and the mechanism of *H. perforatum* L. extract-mediated sustainable synthesis of Ag NPs. Among the phytochemicals present in the extract, it was shown that phenolic acids and flavonoids are employed in the reduction of Ag^+ ions, whereas xanthones and phloroglucinols act as capping agents, and naphthodianthrones are involved in both steps. Tuning the available concentration of these compounds, the NPs can be stabilized sooner or later, leading to the formation of smaller or larger particles. Thus, by varying the ratio between the reducing and capping agents, the size and probably other physicochemical properties of the NPs could be controlled, overcoming a major limitation in green synthesis of NPs. In fact, there is evidence in the literature wherein smaller Ag NPs were synthesized using a higher concentration of compounds that are responsible for nucleation[45,46] Interestingly, the ability to elute the low polar capping agents adsorbed on the surface of NPs with organic solvents in significant quantities opens a new window of application for the easy and quick method for the isolation of valuable drugs and secondary metabolites from complex plant extracts, which is otherwise tedious and time-consuming. Overall, the present study uncovered the phytochemical basis of plant extract and demonstrated a clear picture for NP formation *via* an eco-friendly and sustainable pathway.

ASSOCIATED CONTENT

Supporting Information

The Supporting Information is available free of charge at https://pubs.acs.org/doi/10.1021/acssuschemeng.1c06960.

(Figure S1) UV−vis spectra of Ag NPs prepared using different fractions after 12 h, (Table S1) LC−MS-based identification of secondary metabolites, (Figure S2) details of mass fragmentation for identified compounds, and (Figure S3) chromatograms of phytochemicals eluted in ethyl acetate, acetone, and ethanol from Ag NPs (PDF)

AUTHOR INFORMATION

Corresponding Author

Gregory Franklin − *Institute of Plant Genetics of the Polish Academy of Sciences, 60-479 Poznan, Poland;* orcid.org/0000-0002-6745-3528; Email: fgre@igr.poznan.pl

Authors

Matam Pradeep − *Institute of Plant Genetics of the Polish Academy of Sciences, 60-479 Poznan, Poland*

Dariusz Kruszka − *Institute of Plant Genetics of the Polish Academy of Sciences, 60-479 Poznan, Poland*

Piotr Kachlicki − *Institute of Plant Genetics of the Polish Academy of Sciences, 60-479 Poznan, Poland*

Dibyendu Mondal − *Institute of Plant Genetics of the Polish Academy of Sciences, 60-479 Poznan, Poland*

Complete contact information is available at: https://pubs.acs.org/10.1021/acssuschemeng.1c06960

Notes

The authors declare no competing financial interest.

■ ACKNOWLEDGMENTS

This work was supported by the National Science Centre (NCN), OPUS Project Reg. No. 2016/21/B/NZ9/01980. D.M. and G.F. acknowledge the NANOPLANT project, which received funding from the European Union's Horizon 2020 research and innovation program under grant agreement no. 856961.

■ REFERENCES

(1) Marslin, G.; Sheeba, C. J.; Franklin, G. Nanoparticles Alter Secondary Metabolism in Plants via ROS Burst. *Front. Plant Sci.* **2017**, *8*, 832.
(2) McShan, D.; Ray, P. C.; Yu, H. Molecular Toxicity Mechanism of Nanosilver. *J. Food Drug Anal.* **2014**, *22*, 116−127.
(3) Le Ouay, B.; Stellacci, F. Antibacterial Activity of Silver Nanoparticles: A Surface Science Insight. *Nano Today* **2015**, *10*, 339−354.
(4) Abou El-Nour, K. M. M.; Eftaiha, A.; Al-Warthan, A.; Ammar, R. A. A. Synthesis and Applications of Silver Nanoparticles. *Arabian J. Chem.* **2010**, *3*, 135−140.
(5) Sharma, D.; Kanchi, S.; Bisetty, K. Biogenic Synthesis of Nanoparticles: A Review. *Arabian J. Chem.* **2015**, DOI: 10.1016/j.arabjc.2015.11.002.
(6) Ajitha, B.; Reddy, Y. A. K.; Reddy, P. S. Enhanced Antimicrobial Activity of Silver Nanoparticles with Controlled Particle Size by PH Variation. *Powder Technol.* **2015**, *269*, 110−117.
(7) Akintelu, S. A.; Folorunso, A. S.; Folorunso, F. A.; Oyebamiji, A. K. Green Synthesis of Copper Oxide Nanoparticles for Biomedical Application and Environmental Remediation. *Heliyon* **2020**, *6*, No. e04508.
(8) Marslin, G.; Siram, K.; Maqbool, Q.; Selvakesavan, R. K.; Kruszka, D.; Kachlicki, P.; Franklin, G. Secondary Metabolites in the Green Synthesis of Metallic Nanoparticles. *Materials* **2018**, 940.
(9) Gupta, M.; Tomar, R. S.; Kaushik, S.; Mishra, R. K.; Sharma, D. Effective Antimicrobial Activity of Green ZnO Nano Particles of Catharanthus Roseus. *Front. Microbiol.* **2018**, *9*, 2030.
(10) Ayodhya, D.; Veerabhadram, G. One-Pot Green Synthesis, Characterization, Photocatalytic, Sensing and Antimicrobial Studies of Calotropis Gigantea Leaf Extract Capped CdS NPs. *Mater. Sci. Eng., B* **2017**, *225*, 33−44.
(11) Shanavas, S.; Priyadharsan, A.; Karthikeyan, S.; Dharmaboopathi, K.; Ragavan, I.; Vidya, C.; Acevedo, R.; Anbarasana, P. M. Green Synthesis of Titanium Dioxide Nanoparticles Using Phyllanthus Niruri Leaf Extract and Study on Its Structural, Optical and Morphological Properties. *Mater. Today: Proc.* **2020**, 3531.
(12) Ajitha, B.; Reddy, Y. A. K.; Lee, Y.; Kim, M. J.; Ahn, C. W. Biomimetic Synthesis of Silver Nanoparticles Using Syzygium Aromaticum (Clove) Extract: Catalytic and Antimicrobial Effects. *Appl. Organomet. Chem.* **2019**, *33*, No. e4867.
(13) Bouafia, A.; Laouini, S. E. Green Synthesis of Iron Oxide Nanoparticles by Aqueous Leaves Extract of Mentha Pulegium L.: Effect of Ferric Chloride Concentration on the Type of Product. *Mater. Lett.* **2020**, *265*, 127364.
(14) Some, S.; Bulut, O.; Biswas, K.; Kumar, A.; Roy, A.; Sen, I. K.; Mandal, A.; Franco, O. L.; İnce, İ. A.; Neog, K.; Das, S.; Pradhan, S.; Dutta, S.; Bhattacharjya, D.; Saha, S.; Das Mohapatra, P. K.; Bhuimali, A.; Unni, B. G.; Kati, A.; Mandal, A. K.; Yilmaz, M. D.; Ocsoy, I. Effect of Feed Supplementation with Biosynthesized Silver Nanoparticles Using Leaf Extract of Morus Indica L. V1 on Bombyx Mori L. (Lepidoptera: Bombycidae). *Sci. Rep.* **2019**, *9*, 14839.
(15) Vanlalveni, C.; Lallianrawna, S.; Biswas, A.; Selvaraj, M.; Changmai, B.; Rokhum, S. L. Green Synthesis of Silver Nanoparticles Using Plant Extracts and Their Antimicrobial Activities: A Review of Recent Literature. *RSC Adv.* **2021**, *11*, 2804−2837.
(16) Virmani, I.; Sasi, C.; Priyadarshini, E.; Kumar, R.; Sharma, S. K.; Singh, G. P.; Pachwarya, R. B.; Paulraj, R.; Barabadi, H.; Saravanan, M.; Meena, R. Comparative Anticancer Potential of Biologically and Chemically Synthesized Gold Nanoparticles. *J. Cluster Sci.* **2020**, *31*, 867−876.
(17) Marslin, G.; Selvakesavan, R. K.; Franklin, G.; Sarmento, B.; Dias, A. C. P. Antimicrobial Activity of Cream Incorporated with Silver Nanoparticles Biosynthesized from Withania Somnifera. *Int. J. Nanomed.* **2015**, *10*, 5955−5963.
(18) Latha, M.; Priyanka, M.; Rajasekar, P.; Manikandan, R.; Prabhu, N. M. Biocompatibility and Antibacterial Activity of the Adathoda Vasica Linn Extract Mediated Silver Nanoparticles. *Microb. Pathog.* **2016**, *93*, 88−94.
(19) Raut, R. W.; Mendhulkar, V. D.; Kashid, S. B. Photosensitized Synthesis of Silver Nanoparticles Using Withania Somnifera Leaf Powder and Silver Nitrate. *J. Photochem. Photobiol., B* **2014**, *132*, 45−55.
(20) Jain, S.; Mehata, M. S. Medicinal Plant Leaf Extract and Pure Flavonoid Mediated Green Synthesis of Silver Nanoparticles and Their Enhanced Antibacterial Property. *Sci. Rep.* **2017**, *7*, 15867.
(21) Karthik, C.; Suresh, S.; Sneha Mirulalini, G.; Kavitha, S. A FTIR Approach of Green Synthesized Silver Nanoparticles by Ocimum Sanctum and Ocimum Gratissimum on Mung Bean Seeds. *Inorg. Nano-Met. Chem.* **2020**, *50*, 606−612.
(22) Garibo, D.; Borbón-Nuñez, H. A.; de León, J. N. D.; García Mendoza, E.; Estrada, I.; Toledano-Magaña, Y.; Tiznado, H.; Ovalle-Marroquin, M.; Soto-Ramos, A. G.; Blanco, A.; Rodríguez, J. A.; Romo, O. A.; Chávez-Almazán, L. A.; Susarrey-Arce, A. Green Synthesis of Silver Nanoparticles Using Lysiloma Acapulcensis Exhibit High-Antimicrobial Activity. *Sci. Rep.* **2020**, *10*, 12805.
(23) Manik, U. P.; Nande, A.; Raut, S.; Dhoble, S. J. Green Synthesis of Silver Nanoparticles Using Plant Leaf Extraction of Artocarpus Heterophylus and Azadirachta Indica. *Results Mater.* **2020**, *6*, 100086.
(24) Santos, S. A. O.; Pinto, R. J. B.; Rocha, S. M.; Marques, P. A. A. P.; Neto, C. P.; Silvestre, A. J. D.; Freire, C. S. R. Unveiling the Chemistry behind the Green Synthesis of Metal Nanoparticles. *ChemSusChem* **2014**, *7*, 2704−2711.
(25) Hemlata; Meena, P. R.; Singh, A. P.; Tejavath, K. K. Biosynthesis of Silver Nanoparticles Using Cucumis Prophetarum Aqueous Leaf Extract and Their Antibacterial and Antiproliferative Activity Against Cancer Cell Lines. *ACS Omega* **2020**, *5*, 5520−5528.
(26) Ahn, E.-Y.; Lee, Y. J.; Park, J.; Chun, P.; Park, Y. Antioxidant Potential of Artemisia Capillaris, Portulaca Oleracea, and Prunella Vulgaris Extracts for Biofabrication of Gold Nanoparticles and Cytotoxicity Assessment. *Nanoscale Res. Lett.* **2018**, *13*, 348.
(27) Khorrami, S.; Zarepour, A.; Zarrabi, A. Green Synthesis of Silver Nanoparticles at Low Temperature in a Fast Pace with Unique DPPH Radical Scavenging and Selective Cytotoxicity against MCF-7 and BT-20 Tumor Cell Lines. *Biotechnol. Rep.* **2019**, *24*, No. e00393.
(28) Öztürk, N.; Tunçel, M.; Potoğlu-Erkara, İ. Phenolic Compounds and Antioxidant Activities of Some Hypericum Species: A Comparative Study with H. Perforatum. *Pharm. Biol.* **2009**, *47*, 120−127.
(29) Zou, Y.; Lu, Y.; Wei, D. Antioxidant Activity of a Flavonoid-Rich Extract of Hypericum Perforatum L. in Vitro. *J. Agric. Food Chem.* **2004**, *52*, 5032−5039.
(30) Kladar, N.; Anačkov, G.; Srđenović, B.; Gavarić, N.; Hitl, M.; Salaj, N.; Jeremić, K.; Babović, S.; Božin, B. S. John's Wort Herbal Teas − Biological Potential and Chemometric Approach to Quality Control. *Plant Foods Hum. Nutr.* **2020**, 390.
(31) Wise, K.; Selby-Pham, S.; Bennett, L.; Selby-Pham, J. Pharmacokinetic Properties of Phytochemicals in Hypericum Perforatum Influence Efficacy of Regulating Oxidative Stress. *Phytomedicine* **2019**, *59*, 152763.
(32) Silva, B. A.; Malva, J. O.; Dias, A. C. P. St. John's Wort (Hypericum Perforatum) Extracts and Isolated Phenolic Compounds Are Effective Antioxidants in Several in Vitro Models of Oxidative Stress. *Food Chem.* **2008**, *110*, 611−619.
(33) Sellamuthu, P. S.; Arulselvan, P.; Kamalraj, S.; Fakurazi, S.; Kandasamy, M. Protective Nature of Mangiferin on Oxidative Stress and Antioxidant Status in Tissues of Streptozotocin-Induced Diabetic Rats. *Int. Scholarly Res. Not.* **2013**, *2013*, 750109.

(34) Orčić, D. Z.; Mimica-Dukić, N. M.; Francišković, M. M.; Petrović, S. S.; Jovin, E. Đ. Antioxidant Activity Relationship of Phenolic Compounds in Hypericum Perforatum L. *Chem. Cent. J.* **2011**, *5*, 34.
(35) Silva, B. A.; Ferreres, F.; Malva, J. O.; Dias, A. C. P. Phytochemical and Antioxidant Characterization of Hypericum Perforatum Alcoholic Extracts. *Food Chem.* **2005**, *90*, 157−167.
(36) Matkowski, A.; Kuś, P.; Góralska, E.; Woźniak, D. Mangiferin - a Bioactive Xanthonoid, Not Only from Mango and Not Just Antioxidant. *Mini-Rev. Med. Chem.* **2013**, *13*, 439−455.
(37) Franklin, G.; Conceição, L. F. R.; Kombrink, E.; Dias, A. C. P. Xanthone Biosynthesis in Hypericum Perforatum Cells Provides Antioxidant and Antimicrobial Protection upon Biotic Stress. *Phytochemistry* **2009**, *70*, 60−68.
(38) Zhang, W.; Kong, J.; Chen, H.; Zhao, H.; You, T.; Guo, Y.; Guo, Q.; Yin, P.; Xia, A. Insights into Plasmon Induced Keto−Enol Isomerization. *Nanoscale* **2020**, *12*, 4334−4340.
(39) Halder, A.; Das, S.; Bera, T.; Mukherjee, A. Rapid Synthesis for Monodispersed Gold Nanoparticles in Kaempferol and Anti-Leishmanial Efficacy against Wild and Drug Resistant Strains. *RSC Adv.* **2017**, *7*, 14159−14167.
(40) Hwang, S. J.; Jun, S. H.; Park, Y.; Cha, S.-H.; Yoon, M.; Cho, S.; Lee, H.-J.; Park, Y. Green Synthesis of Gold Nanoparticles Using Chlorogenic Acid and Their Enhanced Performance for Inflammation. *Nanomedicine Nanotechnol., Biol. Med.* **2015**, *11*, 1677−1688.
(41) Rajendran, I.; Dhandapani, H.; Anantanarayanan, R.; Rajaram, R. Apigenin Mediated Gold Nanoparticle Synthesis and Their Anti-Cancer Effect on Human Epidermoid Carcinoma (A431) Cells. *RSC Adv.* **2015**, *5*, 51055−51066.
(42) Oueslati, M. H.; Tahar, L. B.; Harrath, A. H. Catalytic, Antioxidant and Anticancer Activities of Gold Nanoparticles Synthesized by Kaempferol Glucoside from Lotus Leguminosae. *Arabian J. Chem.* **2020**, *13*, 3112−3122.
(43) Bharathi, D.; Bhuvaneshwari, V. Synthesis of Zinc Oxide Nanoparticles (ZnO NPs) Using Pure Bioflavonoid Rutin and Their Biomedical Applications: Antibacterial, Antioxidant and Cytotoxic Activities. *Res. Chem. Intermed.* **2019**, *45*, 2065−2078.
(44) Sudhasree, S.; Shakila Banu, A.; Brindha, P.; Kurian, G. A. Synthesis of Nickel Nanoparticles by Chemical and Green Route and Their Comparison in Respect to Biological Effect and Toxicity. *Toxicol. Environ. Chem.* **2014**, *96*, 743−754.
(45) Bindhu, M. R.; Umadevi, M.; Esmail, G. A.; Al-Dhabi, N. A.; Arasu, M. V. Green Synthesis and Characterization of Silver Nanoparticles from Moringa Oleifera Flower and Assessment of Antimicrobial and Sensing Properties. *J. Photochem. Photobiol., B* **2020**, *205*, 111836.
(46) Molina, G. A.; Esparza, R.; López-Miranda, J. L.; Hernández-Martínez, A. R.; España-Sánchez, B. L.; Elizalde-Peña, E. A.; Estevez, M. Green Synthesis of Ag Nanoflowers Using Kalanchoe Daigremontiana Extract for Enhanced Photocatalytic and Antibacterial Activities. *Colloids Surf., B* **2019**, *180*, 141−149.

https://doi.org/10.1021/acssuschemeng.1c06960
ACS Sustainable Chem. Eng. 2022, 10, 562−571